

Short Communication

## Characterization and Corrosion Behavior of Multilayer [TiAlN]<sub>n</sub> Growth on AISI 316LVM Steel

W. Aperador<sup>1,\*</sup>, G. Roa-Rodríguez<sup>1</sup>, A. Mejía<sup>2</sup>

<sup>1</sup> Department of Mechatronics Engineering, Universidad Militar Nueva Granada, Bogotá D.C., Colombia

<sup>2</sup> Escuela Colombiana de Ingeniería Julio Garavito, Bogotá D.C., Colombia

\*E-mail: [g.ing.materiales@gmail.com](mailto:g.ing.materiales@gmail.com)

Received: 28 March 2014 / Accepted: 15 May 2014 / Published: 16 June 2014

---

In this article was characterized and evaluated the corrosion behavior of [TiAlN]<sub>n</sub> multilayer coatings with 1, 16 and 32 bilayer periods deposited by the magnetron Sputtering PVD technique on stainless steel AISI 316 LVM. The electrochemical behavior that emulated the corporal environment was evaluated by electrochemical impedance spectroscopy using as electrolyte Hank's solution. After the degradation test, the characterization was performed by scanning electron microscopy (SEM) and the corrosion products were evaluated using X ray diffraction. It was found a remarkable increase of the corrosion resistance with the deposition of multilayer coatings on substrates, evidencing the effect of increase the bilayers in the decrease of the degradation when increasing the polarization resistance of the multilayer coatings, corroborating the good performance of the bilayers period variation.

---

**Keywords:** biomaterials, corrosion, multilayers, characterization, Bode Diagram.

### 1. INTRODUCTION

The stainless steel AISI 316 LVM is a biomaterial most used for the manufacturing of temporary implants.[1-3] However, it presents limitations for permanent implants due to the metallic ion liberation towards the surrounding tissues, which increases the risk of developing local tumors, mechanical failure of the implant, DNA damage and alterations associated to cancer etiology.[4] The above limitations lead to focus attention on the search of other materials and/or modify superficially the metallic implants in order that can satisfy the required specifications in bone replacements and decreased ion release. As used strategy to diminish the ions release is the superficial modification of the implants by coatings.[5-6]

Nowadays, the hard coatings such as the nitrides based on transition metals deposited by techniques like physical vapor deposition on different steel substrates, are becoming in the solution of many engineering problems and among them the corrosion, due that these coatings have chemical inertness.[7-8] Among the mentioned nitrides, we have the titanium nitride (TiN) that deposited as monolayer keeps a dominant position in the hard coatings field to improve the wear resistance.[9-10] The properties can be increased by the inclusion of a third component called titanium aluminum nitride (TiAlN), the incorporation of aluminum atoms (Al) inside the crystalline structure of the titanium nitride (TiN) not just increases the oxidation resistance by means of the stable layer formation and compact on the surface, but also contributes to a significant increase of the hardness in comparison with the simple binary nitride.[11-13] In the last years, considerable efforts had performed to develop multicomponents coatings as heterostructures in multilayers with the purpose of improve the wear and oxidation resistance of the coated components. The improvements are presented in the alternated deposition of two or more chemical layers and/or mechanically different, in a way that stress concentration and the conditions to nano-cracks propagation can be controlled. Therefore, the multilayer structure can act as inhibitor of nanocracks, and increase the fracture resistance as well.[12]

The biocompatibility of a material includes all the reactions and effects that take place between the implant and the human body.[4] The initial phase of the contact is associated with the fluid interaction such as blood, saliva or extracellular fluids, producing an adsorption of macromolecules from the fluid toward the implant surface.[5] Normally in this process the proteins are involved, the adsorption of them plays a crucial role in the mechanism of biocompatibility, due to it is bonded with the direct interactions that are produced in the interface.[7]

On the other hand, the human body exerts an influence on the material causing a change in its characteristics, owing to the corrosion and degradation processes mainly. Furthermore, the presence of the material leads to changes in the surrounding tissues through inflammatory processes.[14-15] In surgical implants, the corrosion can be a critic phenomenon that affects the biocompatibility as well as the structural integrity of the prosthesis.[16] The corrosion and dissolution of the superficial layers of the material, both are mechanisms that can derivate a metallic ions introduction in the human body, causing adverse effects by their biological reaction.[17]

In this work was studied the electrochemical behavior of the 316 LVM steel coated with TiAlN, using as simulated biological fluid Hank's solution. We determinate the characteristic of the superficial layer generated in a physiological environment, with the purpose to control the potential toxicity of the metallic ions release in the organism.

## 2. EXPERIMENTAL DEVELOPMENT

[TiAlN]<sub>n</sub> multilayers were deposited on AISI 316 LVM substrates, which were cleaned by ultrasound in an ethanol and acetone sequence during 20 minutes each one. The coatings were obtained by the multi-target magnetron sputtering in r.f (13.56 MHz). For the deposition of the coatings, targets of Ti and Al were used with a purity of 99.9% and diameter of 4 inches. The base pressure at the vacuum chamber interior was  $7.0 \times 10^{-6}$  mbar. Before of initiate the deposition, the

substrates were subjected to plasma cleaning during 20 minutes in Ar atmosphere at bias de -400V in r.f. During the growth, the working gases were a mixture of Ar (93%) and N<sub>2</sub> (7%) with a total working pressure of  $6 \times 10^{-3}$  mbar, at a substrate temperature of 300 °C and a bias r.f of the substrate of -70V. For the multilayers deposition, the aluminum target was covered by the shutter periodically, while the substrate was kept under rotation in front of the targets to facilitate the formation of coatings.

With the purpose to study the influence of the electrochemical behavior of the multilayer coatings, [TiAlN]<sub>n</sub> systems were deposited with periods of 2, 16 and 32 bilayers controlling the times of opening and closing of the shutter. The thickness of the coatings was obtained by a DEKTAK 8000 perfilometer with a peak diameter of 12 μm at a scanning length among 1000 - 1200 μm. For the 2 bilayer specimen, the thickness was  $3.22 \pm 0.04$  μm, and given that the coatings were obtained by the same growth parameters and the total time deposition, is possible to state that the multilayer systems have a thickness around this value.

For the corrosion resistance evaluation at static conditions, was used a potentiostat-galvanostat, Gamry PCI-4 model. Electrochemical impedance spectroscopy (EIS) tests were performed at a temperature of  $37 \pm 0.2$  °C (temperature of the human body at normal conditions), using as electrolyte Hank's solution (Hank's balanced salt solution, Sigma) which chemical solution is detailed in the table 1, the tests were performed in time fuction at 0, 24, 48, 72 and 168 hours. For the mounting was used a cell composed by a counter-electrode of platinum, a reference electrode of Ag/AgCl and a working electrode of 316 LVM alloys coated in an exposed area of 1 cm<sup>2</sup>. The Nyquist diagrams were obtained doing a frequency scans in a range of 0.01 Hz to 100 kHz, using a sinusoidal amplitude signal of 10 mV.

**Table 1.** Chemical composition of the electrolyte (Hank's solution).

Compound	Concentration (gL <sup>-1</sup> )
NaCl	8
D-Glucose	1
MgSO <sub>2</sub> ·7H <sub>2</sub> O	0.7
Na <sub>2</sub> HPO <sub>4</sub>	0.48
KCl	0.4
NaHCO <sub>3</sub>	0.35
CaCl <sub>2</sub> ·H <sub>2</sub> O	0.18
MgO <sub>2</sub> ·6H <sub>2</sub> O	0.08
KH <sub>2</sub> PO <sub>4</sub>	0.06

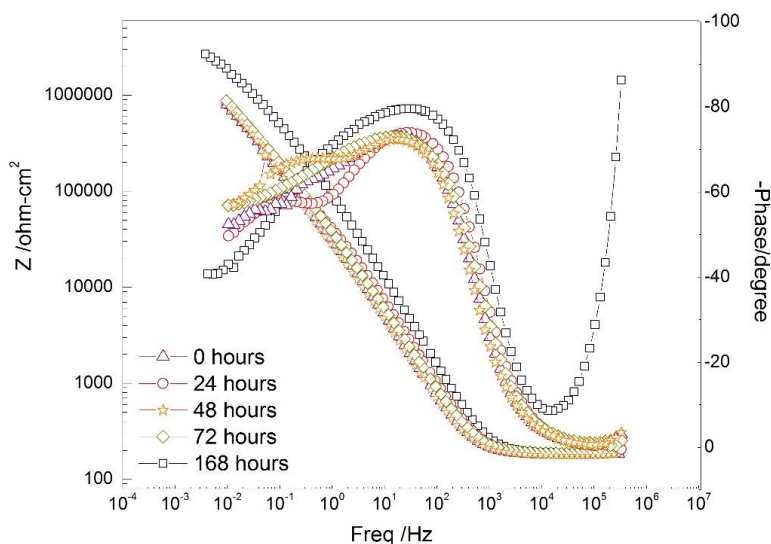
The technique of scanning electron microscopy (SEM) with a resolution of 1-nm a 30 kV allows the microstructural study at the 0 and 168 hours of exposition. The corrosion products generated on the steels surface were identificated by X-ray diffraction (DRX). The experimental arrangement of X-ray diffraction corresponds to a PW3050/60 (θ/θ) goniometer, managed under a XPERT-PRO system using monochromatic radiation of Cu Kα 1.54 Å, working at 40 kV and 40 mA

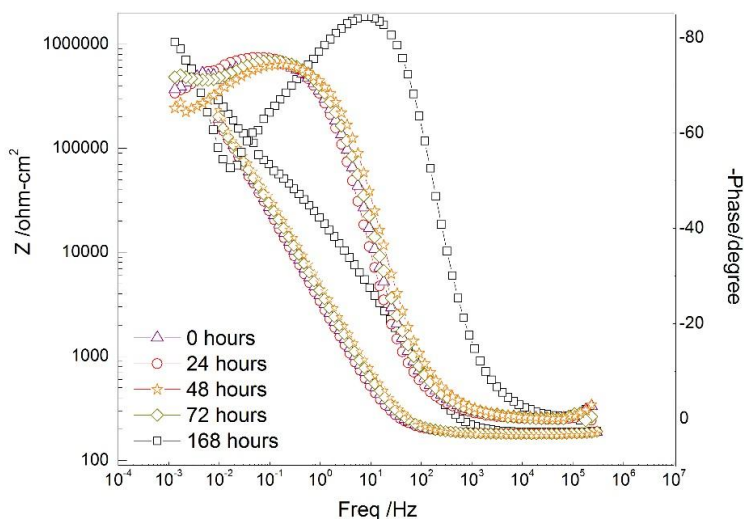
under temperature conditions of 25°C. The scanning on the surface was performed from  $2\theta = 20.01^\circ$  towards  $2\theta = 99.99^\circ$  with a step  $2\theta = 0.02^\circ$  at a scanning time of 1 second.

### 3. RESULTS AND DISCUSSION

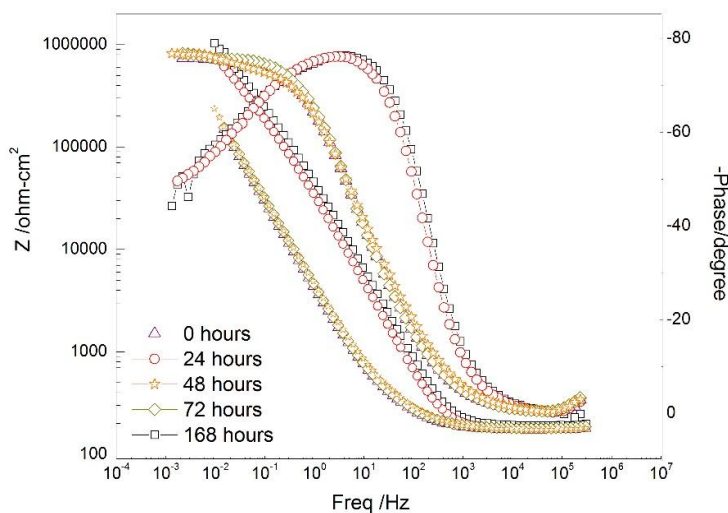
#### 3.1. Electrochemical evaluation

In the figures 1a, 1b and 1c is observed the Bode diagrams for the multi-layer coatings of TiAlN with periods of 1, 16 and 32 bilayers immersed in the biologic fluid in time function performing evaluations at 0, 24, 48, 72 and 168 hours, provided to the response application of the electrochemical impedance spectroscopy (EIS) to evaluate the Hank's solution action on the solution coating interface. The phenomena happen over the time, the material indicate the increasing of the protector effect after the 0 hours of exposition.[19] The behavior in which is appreciated the semicircle formation at high frequencies, is associated to activation phenomena on the metal. This due to the corrosion products formation from the dissolution of the metal through the time (0 to 168 hours), by the effect of the activity of the solution on the thin film that generates a initial degradation. The  $R_2$  of the coating on the coating has higher corrosion resistance at the 0 hours. The  $\log f$  in function of the phase angle shows two inflections for the TiAlN, which indicates the presence of two interfaces; coating/electrolyte and substrate/electrolyte due to the pitting corrosion of the thin film. The electrochemical reactions that occur after the evaluated 0 hours generate a decreasing of the resistances of the systems; this behavior is similar for the three multilayer systems. For that reason, the interface heterogeneity increases, which favor the corrosive processes, due that after 24 hours of evaluation for  $n=2$  and  $n=16$  the system is stabilized, the same behavior is obtained for the system with  $n=32$  at the 24 hours. Comparing, the impedance magnitude of the coating/electrolyte and substrate/electrolyte are lower as time progresses due to the generated corrosion since favor the electrolyte and the coating/electrolyte interface conductivity.[20]





B



C

**Figure 1.** Bode multilayers of [TiAlN] n evaluated at 0, 24, 48, 76 and 168 h, a) n = 1, b) n = 16 and c) n = 32.

When the interfaces is affected and accumulate on the thin film surface, the electrons interchange is accelerated causing an increase in the corrosion velocity. In all of the Bode diagrams showed in the figure 1 is observed a capacitive behavior at high frequencies, in that a flattened semicircle which center is bellow of the real axis. This phenomenon is associated with dispersion in frequency process, due to the surface of the electrode is not homogeneous. In addition, it is observed a diffusion process that pretend to define a second semicircle at low frequencies.[21]

The equivalent circuit that adjusts for the evaluated coatings is shown in the figure 2. The  $CPE_1-R_1$  couple, which predominates at high frequencies, may be originated by the passive film and/or the dielectric properties of the multilayers, while the  $CPE_2-R_2$  couple, controlling at low frequencies, characterizes the corrosion process of the steel/multilayers pore solution interface.  $R\Omega$  is the

electrolyte resistance. The distributions of CPEs are widely used in data fitting because allow analyzed the depressed semicircles. The depressed semicircle is generally due to a dispersion in the time constant, caused by irregularities on the steel surface, surface roughness, fractal surface, and in general certain processes associated with an irregular distribution of the applied potential (10 mV) to obtain EIS data. The admittance representation of a CPE shows a dependent fractional-power on the angular frequency ( $\omega$ ):  $Y_{CPE} = Y_P(j\omega)^\alpha$  where  $Y_P$  is a real adjustable constant used in the non-linear least squares (NLLS) fitting, and  $-1 < \alpha < 1$  is defined as a CPE power.<sup>19</sup> When  $\alpha = 0$ , CPE is a resistor; when  $\alpha = 1$ , it is an ideal capacitor; and when  $\alpha = -1$ , it is an inductor. Finally, if  $\alpha = 0.5$ , CPE is the Warburg admittance.

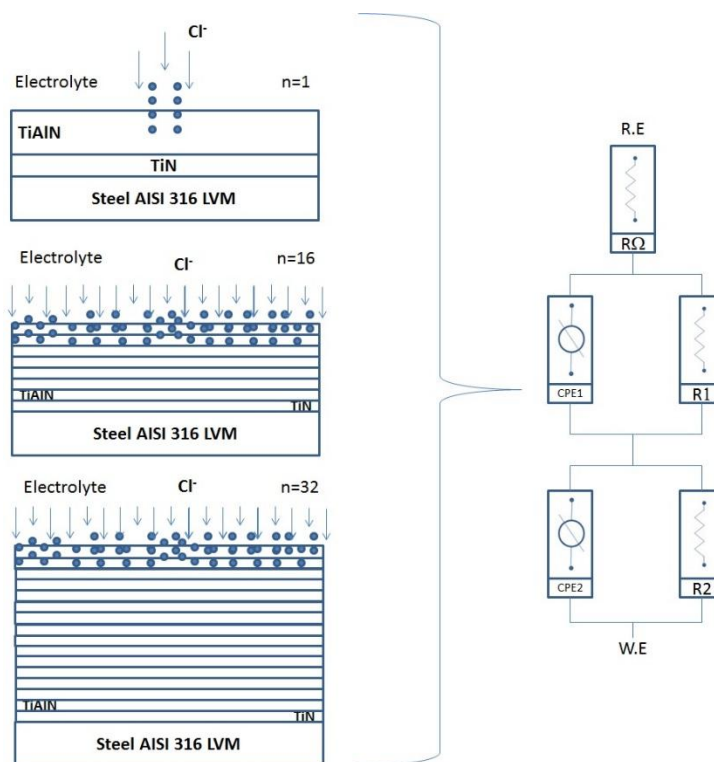


**Figure 2.** Corrosion mechanism proposed for multilayers [TiAlN]<sub>n</sub> and equivalent circuits used for simulation of the experimental data in electrochemical characterization of [TiAlN]<sub>n</sub> multilayers; reference electrode (Re), electrolyte resistance (RΩ), polarization resistance (R1) (films), constant phase elements (CPE), working electrode (WE).

The table 2 shows, is observed the equivalent circuit values in where was obtained the magnitudes of the representative electronic elements of the electrochemical system, these values of mentioned parameters have been obtained by a non-linear program of complex least squares (CNLS). The  $\alpha$  values (table 2), corresponding to the exponential coefficient of the phase angle shift ( $\pi/2$ ); the  $\alpha$  values for the CPE at high values of frequency are in a range of 0.61 y 0.83, which indicates that the rugosity of the surface generates a load distribution, for the CPE at low frequencies shows a  $\alpha$  range, of 0.69 and 0.78 for  $n=1$ ; 0.85 and 0.92 for  $n=16$  and 0.89 and 0.93, indicating that there are migration or diffusion of species, for both  $n=1$ ,  $n=16$  and for  $n=32$  the  $\alpha$  values generate a density distribution of the charge carrier, i.e. a double layer with complex structure.

**Table 2.** Electrochemical parameters obtained by EIS for the coatings after 0, 48, 72 and 168 hours.

<b>n=1</b>							
	$R_{\Omega}$	$CPE_1$		$R_1$	$CPE_2$		$R_2$
	$\Omega \text{ cm}^2$	$\mu\text{F cm}^{-2}$ $s^{-(1-\alpha_1)}$	$\alpha_1$	$10^3\Omega \text{ cm}^2$	$\mu\text{F cm}^{-2}$ $s^{-(1-\alpha_2)}$	$\alpha_2$	$10^6\Omega \text{ cm}^2$
0 hours	165.23 (3%)	1.25 (2%)	0.63 (0.2%)	4,42 (5%)	17.22 (2%)	0.72 (0,6%)	59,46 (6%)
24 hours	185.3 (2%)	2.75 (1.8%)	0.63 (0.3%)	3.03 (3%)	14.74 (4%)	0.69 (0.4%)	42.41 (5%)
48 hours	179.3 (3%)	5,54 (2.9%)	0.64 (0.3%)	3.21 (4%)	13.24 (2%)	0.78 (0.5%)	38.91 (4%)
72 hours	188.8 (4%)	5.67 (2.4%)	0.68 (0.3%)	2.87 (3%)	12.54 (3%)	0,74 (0.7%)	37.98 (3%)
168 hours	177.3 (3%)	5.88 (2.9%)	0.61 (0.3%)	2.85 (4%)	12.35 (5%)	0.72 (0.5%)	37.78 (3%)
<b>n=16</b>							
	$R_{\Omega}$	$CPE_1$		$R_1$	$CPE_2$		$R_2$
	$\Omega \text{ cm}^2$	$\mu\text{F cm}^{-2}$ $s^{-(1-\alpha_1)}$	$\alpha_1$	$10^3\Omega \text{ cm}^2$	$\mu\text{F cm}^{-2}$ $s^{-(1-\alpha_2)}$	$\alpha_2$	$10^6\Omega \text{ cm}^2$
0 hours	176.4 (3%)	31.76 (2%)	0.69 (0.2%)	9,64 (3%)	872.22 (4%)	0.92 (0,6%)	164.34 (4%)
24 hours	181.6 (3%)	2.75 (1.8%)	0.76 (0.6%)	5.13 (3%)	89.67 (3%)	0.91 (0.5%)	76.54 (5%)
48 hours	181.4 (2%)	5,04 (4%)	0.69 (0.3%)	3.54 (2%)	65.18 (2%)	0.87 (0.4%)	72.32 (3%)
72 hours	179.7 (4%)	5.18 (3%)	0.74 (0.2%)	3.66 (4%)	56.68 (2%)	0.85 (0.3%)	69.76 (2%)
168 hours	182.4 (2%)	7.36 (2%)	0.75 (0.4%)	4.47 (3%)	45.19 (2%)	0.87 (0.2%)	66.97 (3%)
<b>n= 32</b>							
	$R_{\Omega}$	$CPE_1$		$R_1$	$CPE_2$		$R_2$
	$\Omega \text{ cm}^2$	$\mu\text{F cm}^{-2}$ $s^{-(1-\alpha_1)}$	$\alpha_1$	$10^3\Omega \text{ cm}^2$	$\mu\text{F cm}^{-2}$ $s^{-(1-\alpha_2)}$	$\alpha_2$	$10^6\Omega \text{ cm}^2$
0 hours	191.3 (2%)	53.21 (4%)	0.62 (0.5%)	16.46 (5%)	921.32 (2%)	0.91 (0.5%)	286.45 (3%)
24 hours	185.6 (2%)	45.65 (2%)	0.76 (0.4%)	15.24 (4%)	843.32 (4%)	0.93 (0.3%)	267.45 (5%)
48 hours	185.6 (3%)	16,34 (2%)	0.73 (0.4%)	6.34 (4%)	134.34 (3%)	0.92 (0.3%)	145.21 (4%)
72 hours	183.6 (5%)	14.21 (4%)	0.79 (0.4%)	6.21 (5%)	126.43 (4%)	0,89 (0.5%)	135.23 (3%)
168 hours	184.6 (3%)	13.32 (3%)	0.83 (0.3%)	6.13 (4%)	121.32 (3%)	0.93 (0.3%)	131.24 (4%)

With relation of the bilayer increasing, is observed that the coated steel with [TiAlN], which contains 32 bilayers shows a widespread displacement to higher polarization resistance values ( $R_2$ ) which correspond to the decreasing of the corrosion current density values, indicating a lower susceptibility to corrosion in the analyzed solution, that can be attributed to the degree of porosity presented, which can produced in the coating by nucleation phenomena during the growth generating a lower resistance path for the Cl ion.

TiAlN coatings due to its high content of Al, are passivated which generates a protector layer that improves the behavior against corrosive phenomena. In the other hand, the corrosion resistance increase with increasing of the period lies in the nature of multilayer structures, inasmuch as by increasing the number of bilayers increases the number of interfaces.[22]

### 3.2. SEM analysis

In the figure 3 is observed the micrographs obtained by scanning electron microscopy, the degradation process of the TiAlN film is evidenced as function of the Hank's solution attack.

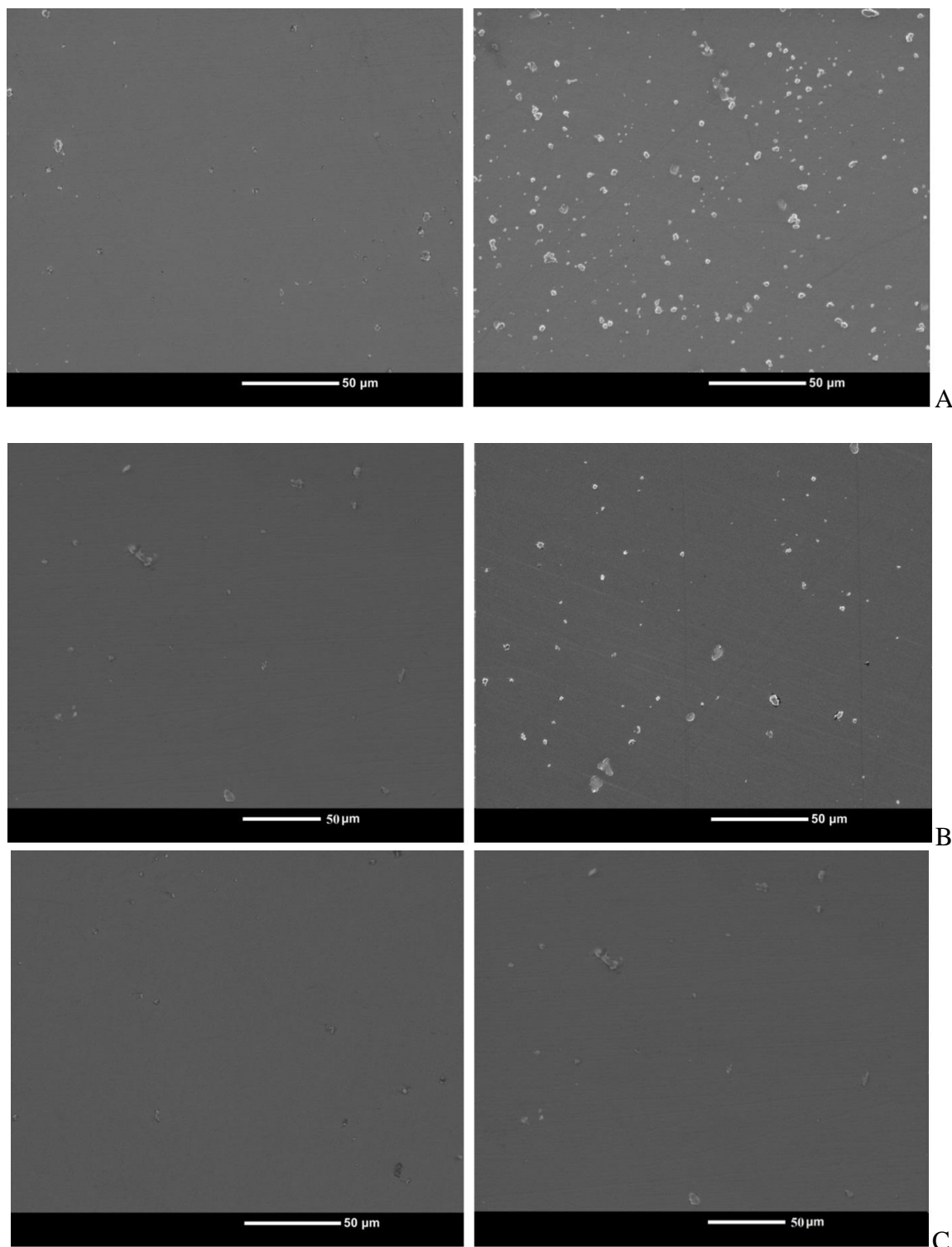


**Figure 3.** Scanning electron microscope of a [TiAlN] n, before (left) and after (right) degradation assay: a) n=1 b) n=16 and c) n=32.

In these images are noticed clearly the superficial attack that suffer the AISI 316 LVM steel substrate with each of the films. The corrosive attack generates a catastrophic damage on the coating surface, moreover generates damages by pitting and breaking of the films continuity as is shown in the figures 3b, 3d 3f increasing drastically the corrosion velocity due to a decrease of the corrosion resistance with the 0 hours of evaluation reference as demonstrated in the EIS analysis.

Finally, it is observed that the deposited film with 32 bilayers (figure 3c) offers higher resistance to the presented attack, thus slightly degraded surface, this behavior is owing to the films with a greater number of bilayers have lower porosity, whose size are smaller as the multilayers increase.

Other characteristic of the micrographs in the figure 3 is that a smooth surface is appreciated, with a porosity of varied in size and even some furrows left by the sanding process of the substrate. With respect to the polarization resistance variation ( $R_2$ ) in function of the immersion time for the different multilayers; in the first 48 hours the resistance has a decrease that can attribute to the localized corrosion generated by the porosity of the coatings. After 72 hours of immersion for the films have stabilization in the electrochemical parameters due to the corrosive attack of the porous zones, corrosion products accumulation in such defects generating the closing of the pores, and the passivation of the coating created by the presence of oxides on the surface.

#### 4. CONCLUSIONS

The corrosion behavior of the velocity with relation the immersion time (168 hours), indicating a stabilization in the coating film, the Change that experience the polarization resistance through the time is appreciated for the Most multilayers in the first immersion hours That the resistance presents a highly value, however at 48 hours this parameter falls, finally remains constant up to 168 hours. This is due to the evolution that the porosity has with the time; a increase in the polarization resistance and hence reducing porosity, which indicates a combination of phenomena: accumulation of corrosion products on such defects and passivation of the substrate and the coating layers. Additionally, it was obtained that increment its protection against degradation phenomena as the number of bilayers increase, then of be in contact with Hank's solution.

Additionally when the multilayers are obtained has been found that it is best to improve their performance in hostile environment generated in the human body which induces an influence on the material causing a change in its characteristics, this was done properly implemented until 32 bilayers which improves its corrosion resistance after being in contact with Hanks solution.

#### References

1. A. J. Van der Borden, H. C. Van der Mei; H. J. Busscher; *Biomaterials*, 26 (2005) 6731.
2. M. Multigner, S. Ferreira-Barragáns; E. Frutos; M. Jaafar; J. Ibáñez; P. Marín; M. T. Pérez-Prado; G. González-Doncel; A. Asenjo; J. L. González-Carrasco; *Surf. Coat. Tech.* 205 (2010) 1830.
3. F. Zivic; F. Babic; N. Grujovic; Mitrovic; D. Adamovic; *Wear.* 300 (2013) 65.
4. S. Karimi; T. Nickchi; A. M. Alfantazi; *Appl. Surf. Sci.* 258 (2012) 6087.

5. H. Farnoush; J. A. Mohandesi; D. A. Fatmehsari; F. Moztaarzadeh; *Ceram. Int.* 38 (2012) 4885.
6. A. Sobczyk-Guzenda; B. Pietrzyk; W. Jakubowski; H. Szymanowski; W. Szymański; J. Kowalski; K. Oleśko; M. Gazicki-Lipman; *Mater. Res. Bull.* 48 (2013) 4022.
7. A. P. Carapeto; A. P. Serro; B. M. F. Nunes; M. C. L. Martins; S. Todorovic; M. T. Duarte; V. André; R. Colaço; B. Saramago; *Surf. Coat. Tech.* 204 (2010) 3451.
8. M. Audronis; Z. M. Rosli; A. Leyland; P. J. Kelly; A. Matthews; *Surf. Coat. Tech.* 202 (2008) 1470.
9. J. C. Caicedo; C. Amaya; G. Cabrera; J. Esteve; W. Aperador; M. E. Gómez; P. Prieto; *Thin Solid Films.* 519 (2011) 6362.
10. J. C. Caicedo; G. Cabrera; H. H. Caicedo; C. Amaya; W. Aperador; *Thin Solid Films.* 520 (2012) 4350.
11. B. Tian; W. Yue; Z. Fu; Y. Gu; C. Wang; J. Liu; *Vacuum.* 99 (2014) 68.
12. A. M. Bolind; A. P. Shivprasad; D. Frazer; P. Hosemann; *Mater. Design.* 52 (2013) 168.
13. W. Aperador; J. C. Caicedo; C. España; G. Cabrera; C. Amaya; *J. Phy. Chem. Solids.* 71 (2010) 1754.
14. B. Kasemo; J. Lausmaa; *Mater. Sci. Eng. C.* 1 (1994) 115.
15. R. Willumeit; J. Fischer; F. Feyerabend; N. Hort; U. Bismayer; S. Heidrich; B. Mihailova; *Acta. Biomater.* 7 (2011) 2704.
16. F. Witte; N. Hort; C. Vogt; S. Cohen; K. U. Kainer; R. Willumeit; F. Feyerabend; *Curr. Opin. Solid. St. M.* 12 (2008) 63.
17. R. A. Antunes; M. C. Lopes de Oliveira; *Acta. Biomater.* 8 (2012) 937.
18. C-C. Chien; K-T. Liu; J-G. Duh; K-W. Chang; K-H. Chung; *Dent. Mater.* 24 (2008) 986.
19. L. Wang; J.F. Su; X. Nie; *Surf. Coat. Tech.* 205 (2010) 1599.
20. D. V. Shtansky; N. A. Gloushankova; A. N. Sheveiko; M. A. Kharitonova; T. G. Moizhess; E. A. Levashov; F. Rossi; *Biomaterials.* 26 (2005) 2909.
21. N. Lin; X. Huang; X. Zhang; A. Fan; L. Qin; B. Tang; *Appl. Surf. Sci.* 258 (2012) 7047.
22. G. Rondelli; P. Torricelli; M. Fini; R. Giardino; *Biomaterials.* 26 (2005) 739.

© 2014 The Authors. Published by ESG ([www.electrochemsci.org](http://www.electrochemsci.org)). This article is an open access article distributed under the terms and conditions of the Creative Commons Attribution license (<http://creativecommons.org/licenses/by/4.0/>).